J Therm Anal Calorim
DOI 10.1007/s10973-017-6373-6

Novel mixed-ligand complexes of coumarilate/*N*,*N*′-diethylnicotinamide with some transition metals

Synthesis and structural characterization

Özge Dağlı[1] · Dursun Ali Köse[1] · Gülçin Alp Avcı[2] · Onur Şahin[3]

Received: 23 November 2016 / Accepted: 26 March 2017

Abstract Coordination complexes of transition metal cations (Co^{II}, Ni^{II}, Cu^{II} and Zn^{II}) containing coumarilate and *N*,*N*′-diethylnicotinamide were synthesized. The structural characterization and thermal behaviour analysis of novel samples synthesized were conducted through elemental analysis, magnetic susceptibility, solid-state UV–Vis, direct and injection probe mass spectra, FTIR spectra, thermoanalytic TG-DTG/DTA and single crystal X-ray diffraction methods. The structural details of single crystals of $[Co(dena)_2(H_2O)_4](coum)_2$ (**I**) and $[Cu(coum)_2(dena)_2(H_2O)_2]$ (**III**) complexes were resolved completely. Moreover, the results of analysis obtained for $[Ni(coum)_2(dena)_2(H_2O)_2]$ (**II**) and $[Zn(dena)_2(H_2O)_4](coum)_2$ (**IV**) complexes were interpreted considering the samples with crystal structures defined and made assumptions about the structural details. It was determined that the complex of Co^{II} metal cation has salt-type structure and the coordination number of metal is accomplished to six as the sum of 4 mol of water and also 2 mol of *N*,*N*′-diethylnicotinamide ligands in trans position located within the coordination sphere. It was observed that 2 mol of coumarilate anions are located outside the coordination sphere and have stabilized to the charge (2+) of metal. The Cu^{II} complex has totally molecular structure, and the coordination sphere of metal cation was 6 as the sum of 2 mol of water, 2 mol of *N*,*N*′-diethylnicotinamide and 2 mol of monoanionic monodentate coumarilate ligands. All ligands have been located in *–trans* position. The geometry of both complex structures is distorted octahedral. It is assumed that the Ni^{II} complex structure is isostructural with Cu^{II} complex structure and also does Zn^{II} complex with Co^{II} structure. It was determined that the decomposition products obtained from thermal analysis are the oxides of related metal cations.

Keywords Coumarilate · *N*,*N*′-diethylnicotinamide · Mixed-ligand–metal complexes · Crystal structure · Thermal analysis · Structural analysis

Introduction

The coumarilic acid (coumarin-3-carboxylic acid, benzo [b] furan carboxylic acid, HCCA, Fig. 1) which is the derivative of coumarin is a ligand that shows monoanionic monodentate or monoanionic bidentate binding features through the carboxylic acid group it has. The benzo [b] furan ring constituting the main body of the structure is available in most of the compounds as a key pharmacophore and can be isolated from the natural sources [1]. It is known that the benzo [b] furan and its derivatives exist in different natural food sources such as fruits, herbs, and vegetables [2]. It is also the major component of the drugs (such as amiodarone and bergapten) synthesized and used in many applications recently [3, 4].

It is well known that many of the heterocyclic compounds containing oxygen in the ring structure exhibit

Electronic supplementary material The online version of this article (doi:10.1007/s10973-017-6373-6) contains supplementary material, which is available to authorized users.

✉ Dursun Ali Köse
dkose@hacettepe.edu.tr

1 Department of Chemistry, Hitit University, 19030 Çorum, Turkey

2 Department of Molecular Biology and Genetics, Hitit University, Ulukavak, Çorum, Turkey

3 Scientific and Technological Research Application Centre, Sinop University, 57000 Sinop, Turkey

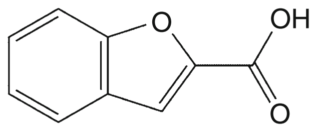

Fig. 1 Coumarilic acid

important biological features such as antiarrhythmic, spasmolytic, antiviral, anticancer, antifungal, and anti-inflammatory activities [5–11]. This group of compounds includes furobenzopyranone, benzofurane and benzopyrano systems.

This feature of coumarilic acid with a good ligand behaviour in terms of coordination chemistry has made many researchers focused on this ligand. There are studies in the literature, in defiance of the limited number, about the complex compound studies performed using metal cations [12–14]. There are also studies showing that the metal complex structures are more effective than ligand structures (without any metal) biologically [15–21].

Although there are many studies conducted using coordination complexes of coumarilic acid containing transition metal cations [14, 22–27], the number of studies on single crystal structure analysis is very limited in amount [1, 25, 26]. Moreover, there is almost no study concerned metal complexes with mixed ligand [1].

Therefore, the conditions of the coordination reaction of coumarilic acid are important, and the researchers adjust the different binding models of ligand ionized (as an anion). Whether the binding of coumarilate ligand as a monodentate-bridge or terminal ligand, or participating in the coordination as bidentate chelator depends on reaction conditions [22–24, 28–30].

The *N*,*N*′-diethylnicotinamide (nikethamide) is one of the nicotinamide (B3 vitamin) derivatives, which is used as a complementary ligand of mixed (ligand) complexes and still used in medical field as a respiratory simulator [31].

The coordination compounds of anionic coumarilic acid and *N*,*N*′-diethylnicotinamide ligands with Co^{II}, Ni^{II}, Cu^{II} and Zn^{II} transition metal cations have been synthesized. The structural features of molecules obtained were characterized using single crystal X-ray diffraction (SC-XRD), UV–Vis, FTIR and solid probe GC–MS methods, and TG-DTG/DTA methods for the determination of thermal behaviour.

Experimental

Materials and methods

The chemicals $Co(NO_3)_2 \cdot 6H_2O$, $Ni(NO_3)_2 \cdot 6H_2O$, $Cu(NO_3)_2 \cdot 3H_2O$, $Zn(NO_3)_2 \cdot 6H_2O$, coumarilic acid and *N*,*Ń*-diethylnicotinamide used in the synthesis of complexes were obtained from the company Sigma-Aldrich. Structural characterizations of these synthesized complexes were characterized by elemental analysis, Fourier Transform Infrared spectroscopy (FTIR), thermogravimetric analysis (TG/DTA), single crystal X-ray diffraction diffractometry (SC-XRD), solid ultraviolet–visible region spectroscopy (S-UV–Vis) magnetic susceptibility and melting point determination methods. The biologic activation studies of the elucidated molecules have been studied in cell culture medium. Bacterial cultures of Enterecoccus faecalis ATCC 29212, Escherichia coli ATCC 25922, Staphylococcus aureus ATCC 25923 and fungal culture of Candida albicans ATCC 10231 were obtained from the culture collection at Hitit University, Faculty of Science and Arts, Departments of Molecular Biology and Genetics/Molecular Microbiology. In this study, nutrient broth and agar (Diffco) for *E. coli*; Tryptone-Yeast extract-Cystine (TYC) broth and agar for *E. fecalis* and *S. aureus*; Eosin Methylene Blue (EMB, Merck) broth and agar for *P. aeroginosa* and Sabouraud Dextrose broth and agar (SD, Merck) for C. albicans were used for growth of microorganisms. All strains stored at −20 °C in appropriate medium containing 10% glycerol and regenerated twice before use.

Synthesis of mixed-ligand complexes

For the synthesis of mixed-ligand complexes, the sodium coumarilate salt was obtained. After dissolving the coumarilic acid of 0.005 mol in a beaker containing 50:50 (v/v) EtOH: H_2O, $NaHCO_3$ of 0.005 mol was added and stirred until the gas evolution was ceased. Following this process, the solution of the neutral ligand *N*,*N*′-diethylnicotinamide (0.005 mol in 25 mL H_2O) was added to the solution obtained and was stirred at room temperature for approximately 30 min. Relevant metal cation nitrate salts in the amount of 0.0025 mol of each was added to the final solution obtained by mixing other two (Scheme 1). The metal salts added in the form of solid were completely dissolved and stirred at 55 °C over a hot plate for 3 h until the solution becomes clear. The clear solutions obtained were allowed to crystallize at room temperature. The precipitated crystals after approximately 3–5 weeks were collected by filtration. The proportions of metal:ligand:ligand for Co, Ni, Cu and Zn transition metal complexes were obtained as 1:2:2 basically.

Results

The elemental analysis results of metal–coumarilate/*N*,*N*′-diethylnicotinamide mixed-ligand complexes are given in Table 1. In addition, the melting point of the complexes,

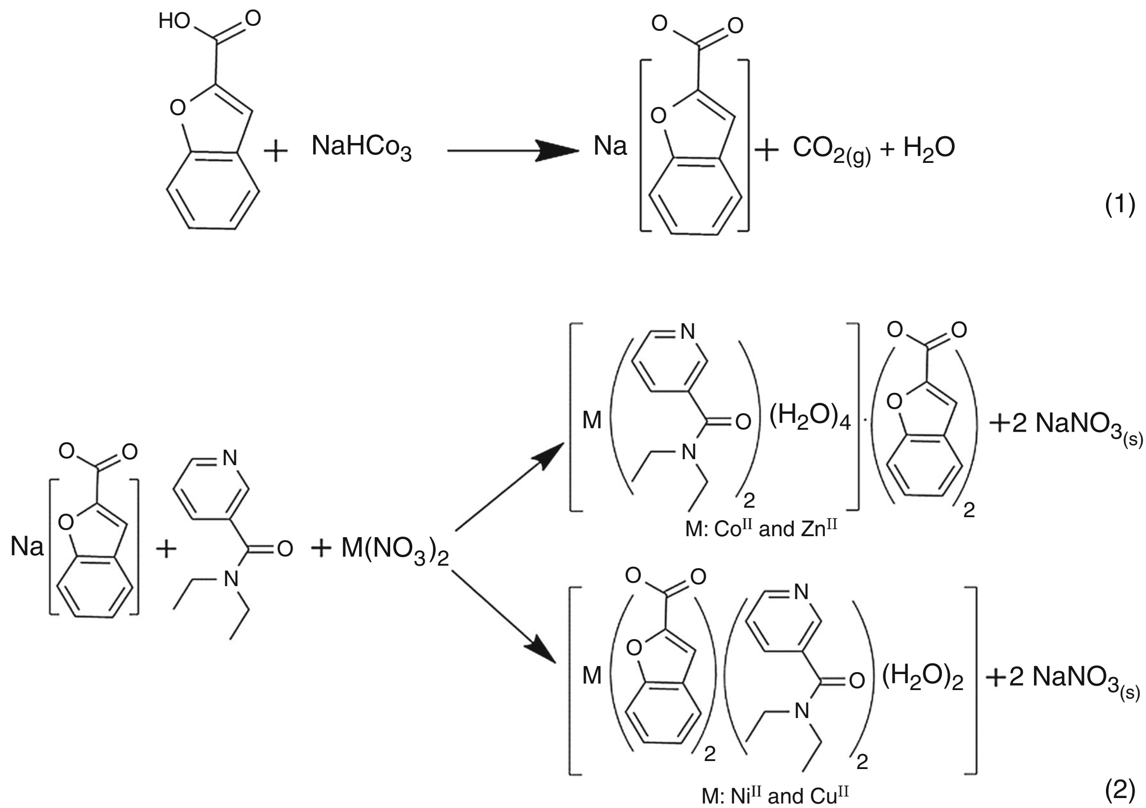

Scheme 1 Reaction of mixed-ligand complexes of coumarilate/*N*,*N*′-diethylnicotinamide

Table 1 Elemental analysis data of metal–coumarilate/*N*,*N*′-diethylnicotinamide mixed-ligand complexes

Complex	Sample mass/g mol^{-1}	Yield	Content/% experimental (theoretical)			Colour	Decomp. temp./K	$\mu_{eff.}$ (BM)
			C	H	N			
$[Co(C_{10}H_{14}N_2O)_2(H_2O)_4](C_9H_5O_3)_2$	809.72	79	20.06	4.26	11.33	Purple	368	4.69
$[Co(dena)_2(H_2O)_4](coum)_2$			(19.74)	(4.94)	(11.52)			
$[Ni(C_9H_5O_3)_2(C_{10}H_{14}N_2O)_2(H_2O)_2]$	773.45	86	20.01	4.67	11.61	Green	380	3.27
$[Ni(coum)_2(dena)_2(H_2O)_2]$			(19.78)	(4.95)	(11.54)			
$[Cu(C_9H_5O_3)_2(C_{10}H_{14}N_2O)_2(H_2O)_2]$	778.29	92	21.24	3.96	12.06	Blue	398	1.79
$[Cu(coum)_2(dena)_2(H_2O)_2]$			(20.90)	(4.36)	(12.13)			
$[Zn(C_{10}H_{14}N_2O)_2(H_2O)_4](C_9H_5O_3)_2$	816.17	87	21.15	4.02	11.46	White	438	dia.
$[Zn(dena)_2(H_2O)_4](coum)_2$			(19.97)	(4.61)	(11.65)			

magnetic susceptibility results, colours and yield estimations can also be seen in the table.

Infrared spectroscopy

The data designating the significant stretching and bending peaks owned by molecules are given in Table 2. The intense and broad band observed near 3600–2900 cm^{-1} is due to the presence of –OH groups in the structure of the complexes. The stretching vibration peaks observed at 1610 cm^{-1} are due to the C=O group of the carboxylic acid in the metal complexes of Co^{II}, Ni^{II} and Cu^{II}, whereas the same peak was observed at 1612 cm^{-1} for Zn^{II} complex. The aromatic C=C stretching vibration was observed at around 3065–3082 cm^{-1}. The aromatic C–H stretching in the complexes has provided stretching vibrations in between 3279 and 3394 cm^{-1}. The COO^- asymmetric and symmetric absorption bands of carboxylic acid were observed at (in order of) 1553–1579 and 1378–1402 cm^{-1}, corresponding to the stretching vibration. The stretching

Table 2 IR spectra of metal–coumarilate/*N*,*N*′-diethylnicotinamide mixed-ligand complexes

Groups	Co^{II}	Ni^{II}	Cu^{II}	Zn^{II}
$\nu(OH)_{H2O}$	3550–2900	3600–2900	3600–2900	3600–2900
$\nu(=C–H)_{aromatic}$	3340	3394	3393	3279
$\nu(C=C)_{aromatic}$	3065	3082	3067	3073
$\nu(CH_2)$	2971, 2931	2973, 2937	2975, 2939	2976, 2933
$\nu(C=O)_{carbonyl}$	1610	1610	1610	1612
$\nu(COO–)_{asym}$	1553	1579	1556	1576
$\nu(COO–)_{sym}$	1389	1402	1378	1400
$\Delta\nu_{as-s}$	164	177	178	176
$\delta(OH)_{H2O}$	1461	1461	1463	1476
$\nu(C–N–C)_{pyridine}$	1334	1343	1338	1329
$\nu(C–O–C)$	1254/1181	1253/1183	1250/1183	1254/1185
$\nu(C–O)_{carboxyl}$	1304	1305	1301	1302
$\nu_{ring\ of\ coumarilate}$	1104–820	1107–832	1104–831	1114–856
$\nu(C–N)_{amide}$	940–704	945–705	943–703	942–706
$\nu(M–N)$	584	589	590	598
$\nu(M–O)$	433	530,427	514,445	431

vibration absorption bands belonging to the metal–oxygen (M–O) binding were observed at 433 cm^{-1} for Co^{II}; 427 and 530 cm^{-1} for Ni^{II}; 445 and 514 cm^{-1} for Cu^{II}; and 431 cm^{-1} for Zn^{II} complexes. The vibrations of metal–nitrogen (M–N) bonds were observed at 584 cm^{-1} for Co^{II}; 589 for Ni^{II}; 590 for Cu^{II}; and 598 cm^{-1} for Zn^{II} [32–34] complexes.

The most significant proof of the monoanionic monodentate binding of carboxylate group is the similarity of the values obtained from the subtraction between the asymmetric and symmetric stretching vibrations of carboxylate and that of sodium salt [31–33, 35]. The corresponding $\nu(COO–)_{asym} - \nu(COO–)_{sym}$ values for Co^{II}, Ni^{II}, Cu^{II} and Zn^{II} structures are 164, 177, 178 and 176 cm^{-1}, respectively. Because the subtraction is below the value of 200 cm^{-1}, the monoanionic monodentate coordination of carboxylate groups has been proved. The existence of two different M–O binding stretching in the complexes **II** and **III** is the proof of both salt-type and coordination bonds. However, the single peak value for the M–O binding in other complex structures may be presented as the confirmation of salt-type binding of coumarilate ligands in the structures as a counter ion. The emerging shift values belonging to the pyridine ring of *N*,*N*′-diethylnicotinamide are the signal of the coordination of the pyridine through nitrogen group.

Solid UV–Vis spectroscopy

The electronic transition values of metal–coumarilate/*N*,*N*′-diethylnicotinamide complexes with mixed ligands were deduced according to the solid phase UV–Vis spectra pattern recorded in the wavelength range of 900–200 nm (Fig. 2). According to these data, *d–d* transitions of Co^{II} complex were observed at the wavelengths of 479.72 ($^4T_{1g} \rightarrow {}^4T_{2g}$) (F) and 450.03 nm ($^4T_{1g} \rightarrow {}^4T_{1g}$) (P). The three spin-allowed *d–d* transitions owned by Ni^{II} complex were corresponded to the wavelengths at 807.12 ($^3A_{2g} \rightarrow {}^3T_{1g}$) (P), 635.39 ($^3A_{2g} \rightarrow {}^3T_{1g}$) (F) and 381.49 nm ($^3A_{2g} \rightarrow {}^3T_{2g}$) (F), and these transition bands provide the

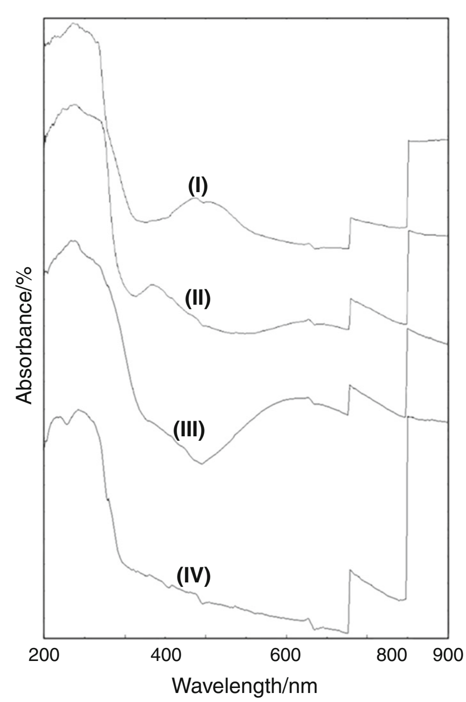

Fig. 2 Solid UV–Vis spectra of complexes

assumption that the *d* orbitals of Ni^{II} metal cations were split to encourage the octahedral geometry. The multi-adsorption band owned by Cu^{II} complex was formed by overlapping peaks and having a broad view in a wide range in between 869.43 and 497.36 nm. The maximum absorption band of the broad spectrum of Cu^{II} complex corresponds to approximately 622.81 nm ($^2E_g \rightarrow {}^2T_{2g}$). Because the *d* orbitals in the last orbital of metal cation of the Zn^{II} complex with a diamagnetic feature detected from the magnetic susceptibility data were fully engaged, there was no any *d*–*d* electronic transition observed during any octahedral split.

The absorption bands observed at a lower wavelength with high intensity do not belong to *d*–*d* transitions, but metal–ligand (M → L) charge transfer with higher energy.

The adsorption bands at 250.67 nm for Co^{II}, 256.21 nm Ni^{II} and 250.51 nm for Cu^{II} complexes do belong to metal–ligand (M → L) transition, whereas the intense peaks observed at the wavelengths of 223.68 and 266.33 nm for Zn^{II} belong to ligand–metal (L → M) charge transfer [36, 37].

Thermal analysis

The thermal analysis curves are shown in Fig. 3, and thermal decomposition steps are summarized in Table 3.

$[Co(C_{10}H_{14}N_2O)_2(H_2O)_4](C_9H_5O_3)_2$: There is four-step decomposition observed at maximum temperatures of 382, 393, 456, 512 K and 587, 625, 661, 774, 918 K available in the DTG curve belonging to (**I**) complex with Co^{II} mixed ligand. Two of the four water ligands in the coordination sphere were removed from the structure at 356–386 K during the first step.

$$\left[Co(C_{10}H_{14}N_2O)_2(H_2O)_4\right](C_9H_5O_3)_{2(s)} \xrightarrow{356-386\,K} \left[Co(C_{10}H_{14}N_2O)_2(H_2O)_4\right](C_9H_5O_3)_{2(s)} + 2H_2O_{(g)} \quad (3)$$

The remaining 2 mol of water ligand in the coordination sphere was completely removed from the structure at decomposition step (120 °C) in the temperature range of 387–436 K.

$$\left[Co(C_{10}H_{14}N_2O)_2(H_2O)_2\right](C_9H_5O_3)_{2(s)} \xrightarrow{387-436\,K} \left[Co(C_{10}H_{14}N_2O)_2\right](C_9H_5O_3)_{2(s)} + 2H_2O_{(g)} \quad (4)$$

The *N*,*N′*-diethylnicotinamide and coumarilic acid ligand of 2 mol each was concurrently removed from the structure in the temperature range of 438–1062 K. The black-coloured CoO compound remained as the decomposition product.

$$\left[Co(C_{10}H_{14}N_2O)_2\right](C_9H_5O_3)_{2(s)} \xrightarrow{438-1062\,K} \left[CoO_{(s)} + 2C_{10}H_{14}N_2O_{(decomp)}\right] + 2C_9H_5O_{3(decomp)} \quad (5)$$

$[Ni(C_9H_5O_3)_2(C_{10}H_{14}N_2O)_2(H_2O)_2]$: It was determined that there are four decomposition steps at maximum

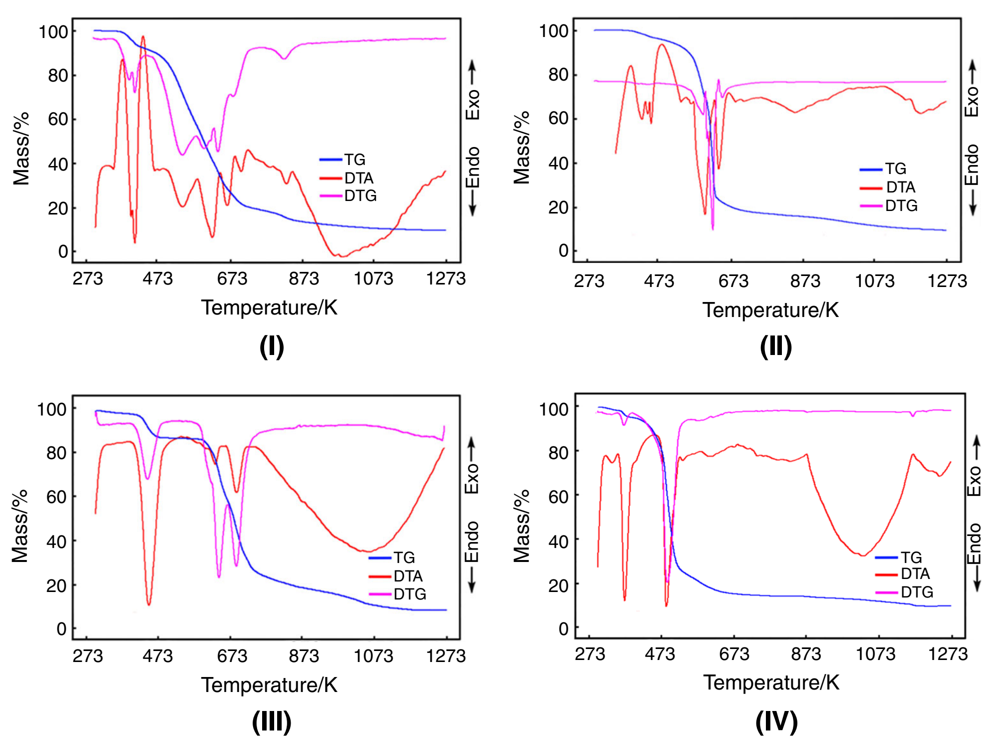

Fig. 3 TG/DTA/DTG curves of complexes; Co^{II} (**I**), Ni^{II} (**II**), Cu^{II} (**III**) and Zn^{II} (**IV**)

Table 3 Thermoanalytical data (TG-DTG/DTA) for the metal complexes

Complex		Temp. range/°C	DTA_{max}/°C	Withdrawing group	Mass/%		Residue/%		Decomp. product	Colour
					Exp.	Theor.	Exp.	Theor.		
$[Co(C_{10}H_{14}N_2O)_2(H_2O)_4](C_9H_5O_3)_2$										Pink
$[Co(dena)_2(H_2O)_4](coum)_2$	1	356–386	382	$2H_2O$	4.22	4.45				
(I)	2	387–436	393	$2H_2O$	4.82	4.45				
809.72 g/mol	3	438–571	456, 512	$2C_{10}H_{14}N_2O$	42.58	43.95				
	4	573–1062	587, 625, 661, 774, 918	$C_9H_5O_2$; $C_9H_5O_3$	36.58	37.81	11.80	9.25	CoO	Black
$[Ni(C_9H_5O_3)_2(C_{10}H_{14}N_2O)_2(H_2O)_2]$										Green
$[Ni(coum)_2(dena)_2(H_2O)_2]$	1	385–423	414	H_2O	2.10	2.33				
(II)	2	424–470	436	H_2O	2.41	2.33				
773.45 g/mol	3	471–591	511, 571	$2C_{10}H_{14}N_2O$	44.82	45.99				
	4	592–1170	606, 647, 670, 797, 1111	$C_9H_5O_2$; $C_9H_5O_3$	37.81	39.60	12.86	9,66	NiO	Black
$[Cu(C_9H_5O_3)_2(C_{10}H_{14}N_2O)_2(H_2O)_2]$										Blue
$[Ni(coum)_2(dena)_2(H_2O)_2]$	1	312–353	332	$H_2O_{(nem)}$	1.26	–				
(III)	2	358–414	368	$2H_2O$	4.25	4.62				
778.29 g/mol	3	416–798	482, 531, 601	$2C_{10}H_{14}N_2O$ $C_9H_5O_2$; $C_9H_5O_3$	77.91	79.50				
	4	901–1218	1028	CO_2	5.12	5.65	11.36	10.22	CuO	Black
$[Zn(C_{10}H_{14}N_2O)_2(H_2O)_4](C_9H_5O_3)_2$										White
$[Zn(dena)_2(H_2O)_4](coum)_2$	1	320–387	366	$H_2O_{(nem)}$	1.23	–				
(IV)	2	390–467	425	$4H_2O$	8.62	8.82				
816.17 g/mol	3	552–635	573, 593	$2C_{10}H_{14}N_2O$	40.97	43.62				
	4	636–1094	648, 985	$C_9H_5O_2$; $C_9H_5O_3$	36.22	37.52	12.96	9.97	ZnO	Grey

temperatures of 414, 436, 511;571 K and 606;647;670;797;1111 K available in the DTG curve belonging to (**II**) complex with Ni^{II} mixed ligand. 1 of 2 mol of water ligand in the coordination sphere was removed from the structure at 385–423 K during the first step.

$$\left[Ni(C_9H_5O_3)_2(C_{10}H_{14}N_2O)_2(H_2O)_{(s)}\right] \xrightarrow{385-423\,K} \left[Ni(C_9H_5O_3)_2(C_{10}H_{14}N_2O)_2(H_2O)\right](s) + H_2O_{(g)} \quad (6)$$

The remaining 1 mol of water ligand in the coordination sphere was completely removed from the structure at the decomposition step (436 K) in the temperature range of 424–470 K.

$$\left[Ni(C_9H_5O_3)_2(C_{10}H_{14}N_2O)_2(H_2O)_{(s)}\right] \xrightarrow{424-470\,K} \left[Ni(C_9H_5O_3)_2(C_{10}H_{14}N_2O)_2\right](s) + H_2O_{(g)} \quad (7)$$

The *N*,*N*′-diethylnicotinamide and coumarilic acid ligand of 2 mol each was concurrently removed from the structure in the temperature range of 471–1170 K. The black-coloured NiO compound remained as the decomposition product.

$$\left[Ni(C_9H_5O_3)_2(C_{10}H_{14}N_2O)_2\right]_{(s)} \xrightarrow{471-1170\,K} \left[NiO_{(s)} + 2C_{10}H_{14}N_2O_{(decomp)}\right] + 2C_9H_5O_{3(decomp)} \quad (8)$$

$[Cu(C_9H_5O_3)_2(C_{10}H_{14}N_2O)_2(H_2O)_2]$: Four decomposition steps are at maximum temperatures of 332, 368, 482;531;601 and 1028 K available in the DTG curve belonging to (**III**) complex with Cu^{II} mixed ligand. The humidity in the structure was removed from the structure at 312–353 K during the first step.

The 2 mol of water ligand in the coordination sphere was completely removed from the structure at the decomposition step (368 K) in the temperature range of 358–414 K.

$$\left[Cu(C_9H_5O_3)_2(C_{10}H_{14}N_2O)_2(H_2O)_2\right]_{(s)} \xrightarrow{358-414\,K} \left[Cu(C_9H_5O_3)_2(C_{10}H_{14}N_2O)_2\right](s) + 2H_2O_{(g)} \quad (9)$$

The *N*,*N*′-diethylnicotinamide and coumarilic acid ligand of 2 mol each was concurrently removed from the structure in the temperature range of 416–798 K.

$$\left[Cu(C_9H_5O_3)_2(C_{10}H_{14}N_2O)_2\right]_{(s)} \xrightarrow{416-798\,K} Cu(CO_3)_{2(s)} + 2C_9H_5O_{3(decomp)} + 2C_{10}H_{14}N_2O_{(decomp)} \quad (10)$$

It is believed that the CO_2 was removed from the structure at the 1028 K decomposition step in the temperature range of 901–1218 K. The black-coloured CuO compound remained as the decomposition end product

$$Cu(CO_3)_{2(s)} \xrightarrow{901-1218\,K} CuO_{(s)} + CO_{2(g)} \quad (11)$$

$[Zn(C_{10}H_{14}N_2O)_2(H_2O)_4](C_9H_5O_3)_2$: The molecule has four decomposition steps at maximum temperatures of 366, 425, 573;593 and 648;985 K available in the DTG curve belonging to (**IV**) complex with the Zn^{II} mixed ligand. It is assumed that the first decomposition step is due to the humidity in the structure at the maximum temperature of 366 K.

The 4 mol of water ligand in the coordination sphere was completely removed from the structure at the decomposition step (425 K) in the temperature range of 390–467 K.

$$\left[Zn(C_{10}H_{14}N_2O)_2(H_2O)_4\right](C_9H_5O_3)_{2(s)} \xrightarrow{390-467\,K} \left[Zn(C_{10}H_{14}N_2O)_2\right](C_9H_5O_3)_{2(s)} + 4H_2O_g \quad (12)$$

The *N*,*N*′-diethylnicotinamide and coumarilic acid ligand of 2 mol each was concurrently removed from the structure in the temperature range of 552–1094 K. The grey-coloured ZnO compound remained as the decomposition product.

$$\left[Zn(C_{10}H_{14}N_2O)_2\right](C_9H_5O_3)_{2(s)} \xrightarrow{552-1094\,K} ZnO_{(s)} + 2C_{10}H_{14}N_2O_{(decomp)} + 2C_9H_5O_{3(decomp)} \quad (13)$$

The decomposition steps of mixed-ligand metal complexes are consistent with the literature, and thermal degradation product-related metal oxides were determined by IR spectra [36–39].

X-ray diffraction analysis

Suitable crystals of **I** and **III** were analysed using a Bruker APEX-II diffractometer equipped with a graphite monochromatic Mo-K_α radiation. The structures were clarified by direct methods using SHELXS-97 and refined by full-matrix least-squares methods on F^2 using SHELXL-97 [40] from within the WINGX [41] suite of software. All non-hydrogen atoms were refined with anisotropic parameters. The H of C atoms were located from different maps and then treated as riding atoms with C–H distances of 0.93–0.97 Å. The water H atoms were located on a different map refined freely. Molecular diagrams were created using the software MERCURY [42]. Supramolecular analyses were performed, and the diagrams were prepared with the aid of PLATON [43]. Details of data collection and crystal structure determinations are given in Table 4.

Complex I: The molecular structure of **I** with atomic label is shown in Fig. 4. The asymmetric unit of **I** contains a Co^{II} ion, a *N*,*N*′-diethylnicotinamide ligand, a non-coordinated coumarilic acid ligand and two aqua ligands. The Co^{II} ion is located on the centre of symmetry and is coordinated by two nitrogen atoms of two *N*,*N*′-diethylnicotinamide ligands and four oxygen atoms from aqua ligands. The coordination geometry around the Co^{II} ion can be described as a distorted octahedral geometry. The Co–O bond lengths are 2.0678 (11) and 2.1034 (11) Å, while the Co–N bond length is 2.1649 (12) Å (Table 5).

Table 4 Crystal data and structure refinement parameters for complexes **I** and **III**

Crystal data	**I**	**III**
Empirical formula	$[Co(dena)_2(H_2O)_4](coum)_2$	$[Cu(coum)_2(dena)_2(H_2O)_2]$
Formula mass	809.72	778.29
Crystal system	Triclinic	Monoclinic
Space group	P-1	$P2_1$
a/Å	7.9249 (5)	8.4196 (6)
b/Å	8.4475 (5)	12.2845 (9)
c/Å	16.6372 (10)	18.2399 (13)
α/°	100.387 (2)	90.00
β/°	92.791 (3)	98.887 (2)
γ/°	113.396 (2)	90.00
V /Å^3	996.50 (11)	1863.9 (2)
Z	1	2
D_c /g cm^{-3}	1.349	1.387
θ range /°	3.2–28.4	3.3–28.0
Measured refls.	46750	54225
Independent refls.	4945	9280
R_{int}	0.027	0.048
S	1.09	1.03
R1/wR2	0.037/0.099	0.037/0.081
$\Delta\rho_{max}/\Delta\rho_{min}$ / eÅ^{-3}	0.54/−0.53	0.33/−0.34

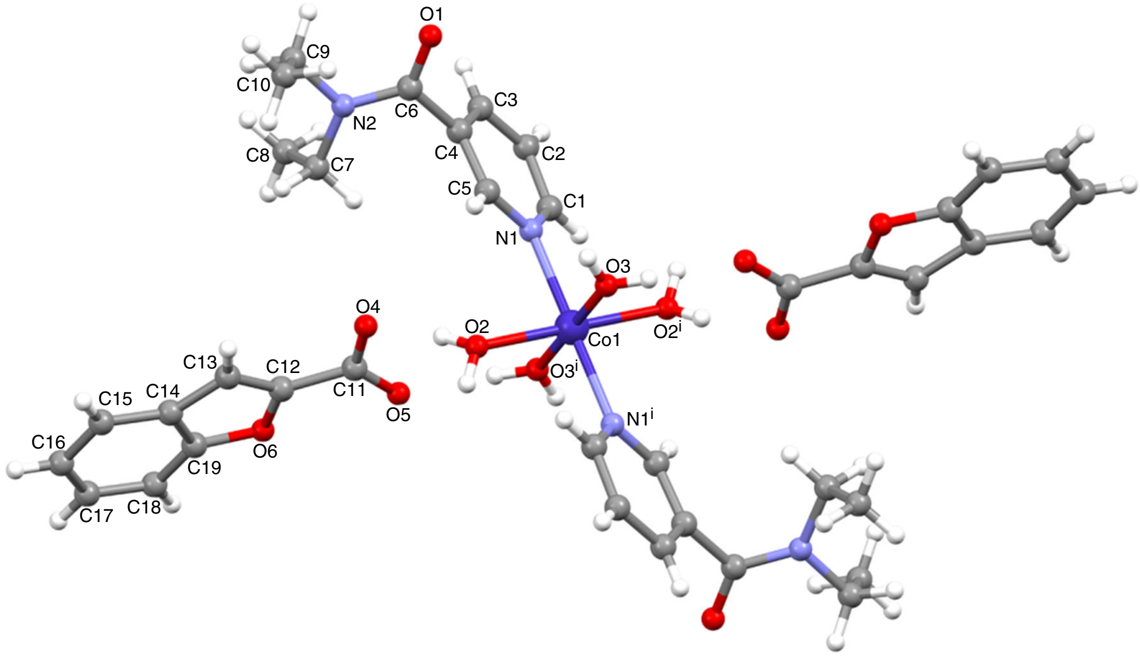

Fig. 4 Molecular structure of complex **I** showing the atom-numbering scheme

Table 5 Selected bond distances and angles for complexes **I** and **III** (Å, °)

*Complex **I***					
N1–Co1	2.1649 (12)	Co1–O2	2.0678 (11)	Co1–O3	2.1034 (11)
O2–Co1–O3	90.11 (5)	O2–Co1–O3^{i}	89.89 (5)	O2–Co1–N1^{i}	92.16 (5)
O2–Co1–N1	87.84 (5)	O3^{i}–Co1–N1^{i}	93.65 (5)	O3–Co1–N1^{i}	86.35 (5)
*Complex **III***					
N1–Cu1	2.012 (2)	N3–Cu1	2.018 (2)	O1–Cu1	1.9679 (19)
O4–Cu1	1.965 (2)	Cu1–O10	2.322 (3)	Cu1–O9	2.729 (2)
O4–Cu1–O1	174.42 (13)	O1–Cu1–N1	89.83 (9)	O4–Cu1–N3	90.75 (10)
O1–Cu1–N3	88.49 (9)	N1–Cu1–N3	172.77 (10)	O4–Cu1–O10	92.76 (10)

Symmetry code: (i) $-x$, $-y + 1$, $-z + 1$ for **I**

The molecule of **I** is linked into the sheets by the combination of O–H···O and C–H···O hydrogen bonds (Table 6). The water O3 atom in the molecule at (x, y, z) acts as a hydrogen bond donor, via atoms H3A and H3B, to atoms O5^{i} and O5^{v}, and thus forms a centrosymmetric $R_4^2(8)$ ring centred at (*n*, 1/2, 1/2) [*n* = zero or integer] [(i) $-x$, $-y + 1$, $-z + 1$; (v) $x - 1$, y, z] (Fig. 5). Similarly, water O2 atom in the molecule at (x, y, z) acts as a hydrogen bond donor, via atom H2A, to atom O1^{iv}, and thus forms centrosymmetric $R_2^2(16)$ ring centred at (0, n, 1/2) [*n* = zero or integer] which is running parallel to the [010] direction [(iv) x, $y - 1$, z] (Fig. 6).

Complex III: The molecular structure of complex **III**, with atom-numbering scheme, is shown in Fig. 7. The asymmetric unit of **III** contains a Cu^{II} ion, two coumarilic acid ligands, two *N*,*N*′-diethylnicotinamide ligands and two water ligands. The coordination geometry of a Cu^{II} ion is a distorted octahedron in which there are two oxygen atoms of two different coumarilic acid ligands, two nitrogen atoms of two *N*,*N*′-diethylnicotinamide ligands and two oxygen atoms from aqua ligands. The Cu–$O_{carboxyl}$ bond lengths are 1.965 (2) and 1.968 (2) Å. The Cu–O_{aqua} bond lengths are 2.322 (3) and 2.729 (2) Å, while the Cu–N bond lengths are 2.012 (2) and 2.018 (2) (Table 5). The O9 atom of aqua ligand is weakly coordinated to the Cu^{II} ion, and the bond is longer than those of the Cu–O bonds due to the Jahn–Teller effect.

Molecules of **III** are linked to the sheets by a combination of O–H···O and C–H···O hydrogen bonds (Table 6). Water O10 atom in the molecule at (*x*, *y*, *z*) acts as a hydrogen bond donor, via atom H10A, to atom O2^{ii}, and thus forms C(6) chain running parallel to the [010]

Table 6 Hydrogen bond parameters for complexes **I** and **III** /Å, °

D–H···A	D–H	H···A	D···A	D–H···A
*Complex **I***				
C2—H2···O5^{ii}	0.93	2.57	3.386 (2)	146
C7—H7B···O4	0.97	2.46	3.241 (3)	137
C18—H18···O4^{iii}	0.93	2.54	3.427 (3)	160
O2—H2A···O1^{iv}	0.82 (2)	1.94 (2)	2.7551 (18)	170 (2)
O2—H2B···O4	0.85 (2)	1.78 (2)	2.6175 (17)	173 (2)
O3—H3A···O5^{v}	0.82 (2)	1.93 (2)	2.7212 (16)	162 (2)
O3—H3B···O5^{i}	0.83 (2)	1.94 (2)	2.7760 (16)	176 (2)
*Complex **III***				
C30—H30···O8^{i}	0.93	2.42	3.297 (4)	158
C36—H36C···O9^{ii}	0.96	2.60	3.514 (7)	159
O9—H9A···O2	0.92 (3)	1.80 (4)	2.645 (5)	151
O9—H9B···O8^{iii}	0.91 (3)	2.01 (4)	2.880 (5)	162
O10—H10A···O2^{ii}	0.86 (2)	1.95 (3)	2.809 (4)	177
O10—H10B···O5	0.83 (2)	1.95 (3)	2.737 (4)	157

Symmetry codes: (i) $-x, -y+1, -z+1$; (ii) $-x+1, -y+2, -z+1$; (iii) $x+1, y, z$; (iv) $x, y-1, z$; (v) $x-1, y, z$ for **I**; (i) $-x+2, y+1/2, -z+1$; (ii) $-x+1, y-1/2, -z+1$; (iii) $-x+1, y+1/2, -z+1$ for **III**

direction [(ii) $-x+1, y-1/2, -z+1$] (Fig. 8). Similarly, water O9 atom in the molecule at (x, y, z) acts as a hydrogen bond donor, via atom H9B, to atom O8^{iii}, and thus forms C(8) chain running parallel to the [010] direction [(iii) $-x+1, y+1/2, -z+1$] (Fig. 9). All of these intermolecular interactions give two-dimensional framework results.

Biological applications

The antimicrobial and antifungal effects of the synthesized metal complexes **I–IV** were determined by the disc diffusion method according to the Clinical and Laboratory Standards Institute (CLSI) guidelines. First, 0.01 g of each of the metal complexes was dissolved in 1 mL dimethylsulphoxide (DMSO). The microorganisms were grown in a suitable broth at 310 ± 1 K for 24 h. All the Mueller-Hinton agar (MHA) plates were prepared with a final depth of 4 mm. Next 0.1 mL suspension of tested microorganisms (10^6 cells mL^{-1}; turbidity = McFarland barium sulphate standard 0.5) was spread on the agar plates. Then, 6-mm-diameter sterile filter paper discs (Whatman, no. 4) were placed on the agar plates and impregnated with 15 µL of metal complexes in DMSO. These plates were incubated at 310 ± 1 K for 24–48 h. DMSO without metal complexes was used as control. Amoxicillin (20 µg) + Clavulanic acid (10 µg), amikacin (30 µg), ampicillin (10 µg), gentamicin (25 µg), nystatin (25 µg) and flucanazole (20 µg) were screened under similar conditions as the standard antibiotic discs. At the end of the incubation period, the inhibition zones around the discs

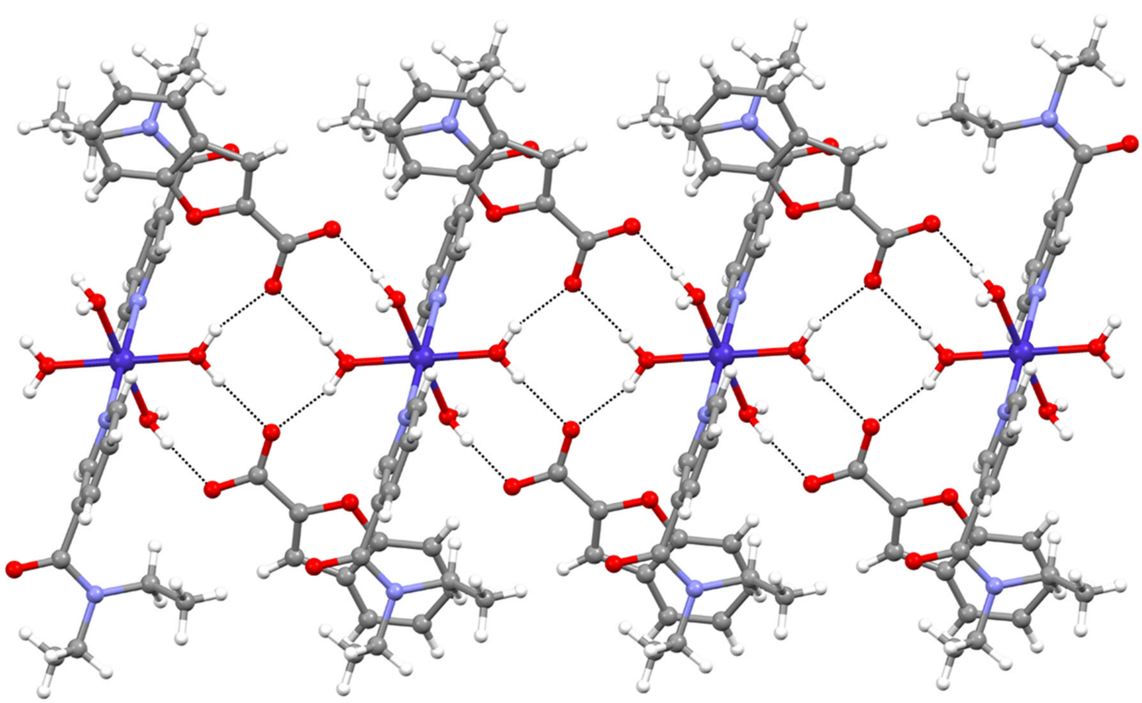

Fig. 5 Formation of edge-fused $R_4^2(8)$ rings in **I**

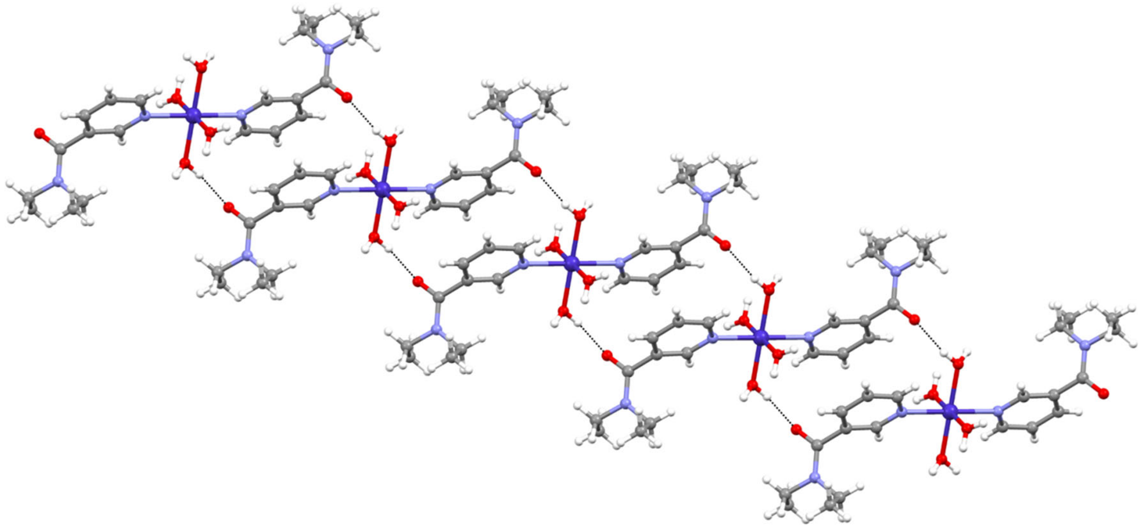

Fig. 6 Formation of edge-fused $R_2^2(16)$ rings in **I**

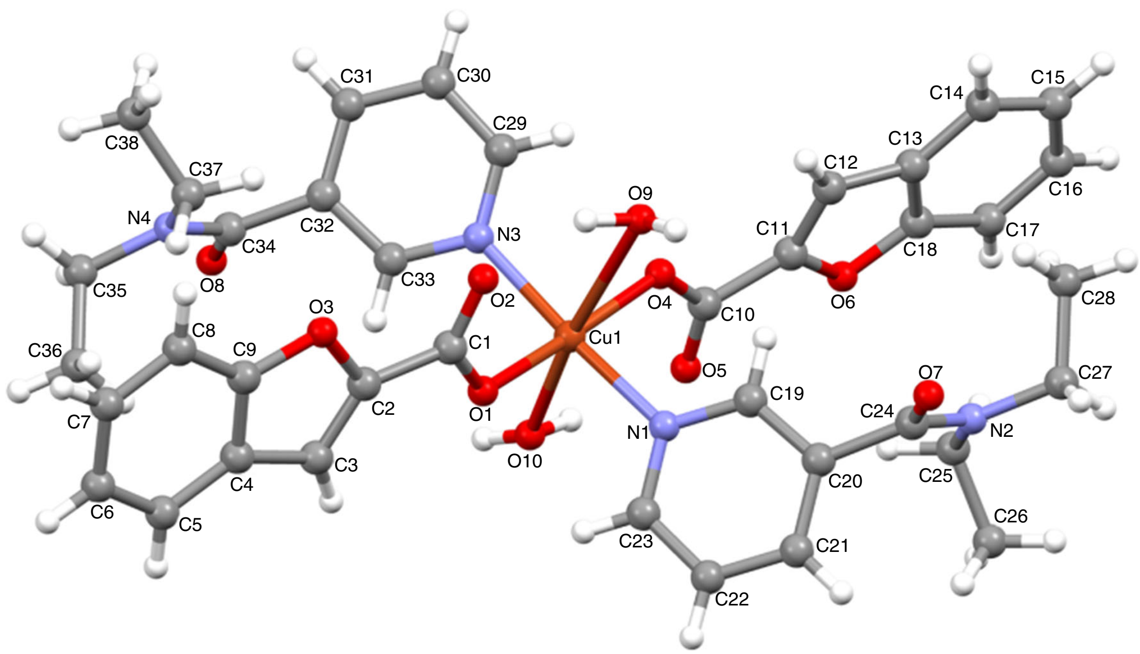

Fig. 7 Molecular structure of complex **III** showing the atom-numbering scheme

were measured as millimetres. The antimicrobial (antibacterial and antifungal) test results of complexes synthesized are given in Table 7.

It was observed that the complexes of **I**, **II**, **III** and **IV** have the antimicrobial effects towards the pathogenic microorganisms on varying proportions. The effects of the synthesized molecules on yeast, gram-positive and gram-negative bacteria were observed. However, it has been found that some mixed ligand complexes have more active activity on specific microorganisms. The inhibitory effects of complexes according to biological applications can be referred as the complex number **I** on *Staphylococcus aureus* ATCC 25923, *Enterococcus faecalis* ATCC 29212 and *Candida albicans* ATCC 10231 and the complex number **II** on *Staphylococcus aureus* ATCC 25923 and *Candida albicans* ATCC 10231. The complexes number **III** and **IV** were observed to have low rate inhibitory effects on all microorganisms except for *Staphylococcus aureus* ATCC 25923. In particular, it is seen that all metal complexes are effective on *Escherichia coli* ATCC 25922 and *Candida albicans* ATCC 10231.

Total Antioxidant Capacity: The total antioxidant capacity (TAC) of the metal complexes was determined according to the procedures described in TAC Assay Kit

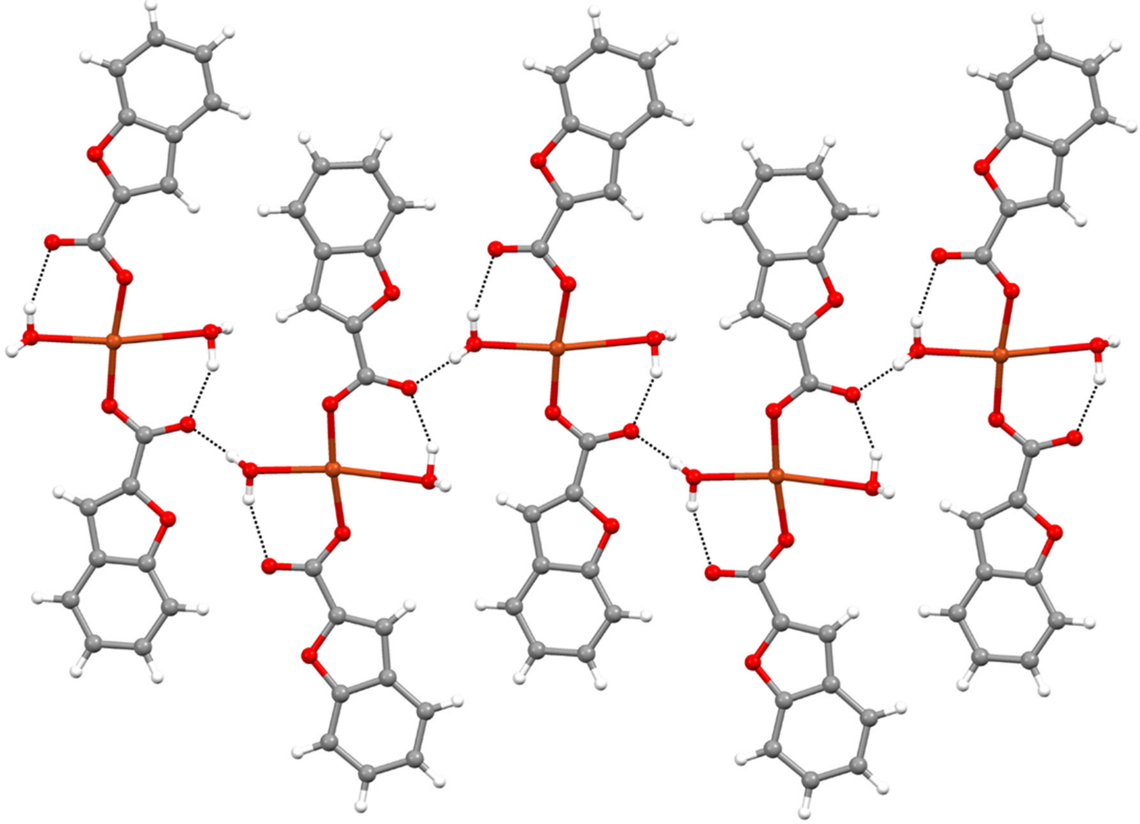

Fig. 8 Formation of C(6) chain in complex **III**

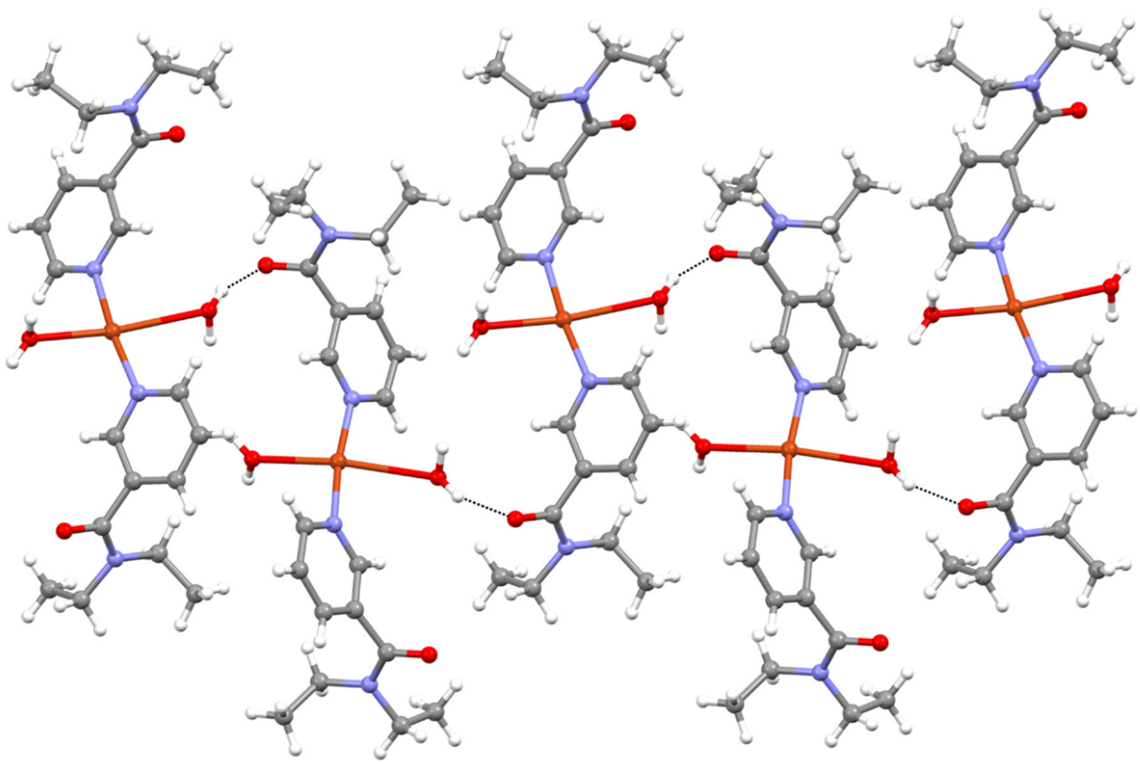

Fig. 9 Formation of C(8) chain in complex **III**

Table 7 In vitro antimicrobial activity test results of metal complexes synthesized

Complexes	Antimicrobial activity (inhibition diameter, mm ± SD)				
	Staphylococcus aureus	*Enterococcus faecalis*	*Escherichia coli*	*Pseudomonas aeroginosa*	*Candida albicans*
I	7. 0 ± 1.0	6.5 ± 0.5	4.0 ± 1.0	ND	7.0 ± 1.0
II	7.0 ± 0.5	4.0 ± 1.0	2.0 ± 0.5	ND	6.0 ± 1.5
III	ND	5.0 ± 1.0	4.5 ± 1.0	3.0 ± 1.0	3.0 ± 0.5
IV	ND	4.0 ± 1.0	3.5 ± 0.5	4.0 ± 1.0	4.0 ± 1.0
AMC	ND	ND	ND	ND	ND
AK	20.0 ± 2.1	20.5 ± 1.0	18.8 ± 2.8	19.8 ± 3.5	ND
AMP	17.4 ± 1.2	16.2 ± 1.3	15.8 ± 1.2	17.7 ± 2.4	ND
GN	9.5 ± 2.0	7.0 ± 1.0	8.75 ± 2.25	10.5 ± 2.5	ND
NYS	ND	ND	ND	ND	17.2 ± 1.2
FL	ND	ND	ND	ND	17.7 ± 1.8

Culture codes of microbial strains; *Enterecoccus faecalis* ATCC 29212, *Escherichia coli* ATCC 25922, *Staphylococcus aureus* ATCC 25923 and *Candida albicans* ATCC 10231

Standards: *AMC* Amoxicillin (20 µg) + Clavulanic acid (10 µg), *AK* amikacin 30 µg), *AMP* ampicillin (10 µg), *GN* gentamicin (25 µg), *NYS* nystatin (25 µg) and *FL* flucanazole (20 µg)

Table 8 Total antioxidant capacity (TAC) of complexes synthesized

Metal complexes	TAC (µmol Trolox Eq/L)
I	1.47
II	1.43
III	1.24
IV	1.91

(Rel Assay Diagnostics®, Turkey). This method is a novel automated colorimetric measurement method developed by Erel (2004) [44]. As a result of this reaction, the bright yellowish-brown dianisyl radical was obtained. Results were expressed as micromolar Trolox equivalents per litre (µmol Trolox Eq/L). The total antioxidant activity (TAC) is given in Tables 7 and 8, respectively.

In the case that we look at the antioxidant activities of the complexes, it is seen that all chemicals generally have a certain amount of activity; especially, the activity of **IV** seems one step ahead.

Conclusions

The studies on the structural conformations of molecules, binding properties and thermal decomposition steps were performed. The metal:ligand:ligand proportions of mixed-ligand complexes were determined as 1:2:2. The complexes of **I** and **IV** were determined to have a salt-type isostructure. It was found that the coumarilate anion is located outside of the coordination sphere as the balancing ions. It was observed that the 4 mol of aqua and 2 mol of *N*,*N*′-diethylnicotinamide ligands bonded as monodentate in the coordination sphere were coordinated to the metal. Moreover, it was confirmed that the structures number **II** and **III** is molecular, and there are also aqua, monodentate *N*,*N*′-diethylnicotinamide and monoanionic monodentate coumarilate ligands with the amount of 2 mol each detected within the coordination sphere. The positions of ligand in the coordinations of all structures have been identified as –*trans*, and the coordination spheres of metal cations were found to have octahedral structure. In addition, the structures have formed the network lattice structures via hydrogen bonding.

The reason for the black colour of decomposition end products identified in all structures at the end of the thermal decomposition and a few higher experimental data of decomposition products as compared theoretical ones can be the carbonized coal remained in the medium without being totally fired depending on the inert nitrogen atmosphere under which the process was carried out.

The electronic transition spectra and the magnetic susceptibility values of the metal cations have encouraged the existence of “pseudo-octahedral” structures due to the Jahn–Teller decomposition effect.

Supplementary material

Crystallographic data for the structural analysis have been deposited with the Cambridge Crystallographic Data Centre, CCDC No. 1465359 for **I** and 1465358 for **III**. Copies of this information may be obtained free of charge from the Director, CCDC, 12 Union Road, Cambridge CB2 1EZ, UK (fax: +44-1223-336033; e-mail: deposit@ccdc.cam.ac.uk or www: http://www.ccdc.cam.ac.uk).

Acknowledgements This study was financially supported by Sinop University in Turkey (Project No. SÜB-1901.14-01). The authors acknowledge Scientific and Technological Research Application and Research Centre, Sinop University, Turkey, for the use of the Bruker D8 QUEST diffractometer. This research was supported by the Science Research Department of Hitit University (Project No: FEF19004.15.005).

References

1. Köse DA, Öztürk B, Şahin O, Büyükgüngör O. Mixed ligand complexes of coumarilic acid/nicotinamide with transition metal complexes. J Therm Anal Calorim. 2014;115(2):1515–24.
2. Kleiner HE, Vulimiri SV, Miller L, Johnson WH, Whitman CP, DiGiovanni J. Oral administration of naturally occurring coumarins leads to altered phase I and II enzyme activities and reduced DNA adduct formation by polycyclic aromatic hydrocarbons in various tissues of SENCAR mice. Carcinogenesis. 2001;22(1):73–82.
3. Tanew A, Ortel B, Rappersberger K, Hönigsmann H. 5-Methoxypsoralen (Bergapten) for photochemotherapy: bioavailability, phototoxicity, and clinical efficacy in psoriasis of a new drug preparation. J Am Acad Dermatol. 1988;18(2):333–8.
4. Gill J, Heel RC, Fitton A. Amiodarone. Drugs. 1992;43(1): 69–110.
5. Hattori M, Hada S, Watahiki A, Ihara H, Shu YZ, Kakiuchi N, et al. Studies on dental caries prevention by traditional medicines. X. Antibacterial action of phenolic components from mace against Streptococcus mutans. Chem Pharm Bull. 1986;34(9): 3885–93.
6. Erber S, Ringshandl R, Von Angerer E. 2-Phenylbenzo [b] furans: relationship between structure, estrogen receptor affinity and cytostatic activity against mammary tumor cells. Anticancer Drug Des. 1991;6(5):417–26.
7. Cui B, Chai H, Santisuk T, Reutrakul V, Farnsworth NR, Cordell GA, et al. Novel cytotoxic 1H-cyclopenta [b] benzofuran lignans from Aglaia elliptica. Tetrahedron. 1997;53(52):17625–32.
8. Kodama I, Kamiya K, Toyama J. Amiodarone: ionic and cellular mechanisms of action of the most promising class III agent. Am J Cardiol. 1999;84(9):20–8.
9. Lee SK, Cui B, Mehta RR, Kinghorn AD, Pezzuto JM. Cytostatic mechanism and antitumor potential of novel 1H-cyclopenta [b] benzofuran lignans isolated from Aglaiaelliptica. Chem Biol Interact. 1998;115(3):215–28.
10. Hwang BY, Su B-N, Chai H, Mi Q, Kardono LB, Afriastini JJ, et al. Silvestrol and episilvestrol, potential anticancer rocaglate derivatives from Aglaia silvestris. J Org Chem. 2004;69(10): 3350–8.
11. Hayakawa I, Shioya R, Agatsuma T, Furukawa H, Naruto S, Sugano Y. 4-Hydroxy-3-methyl-6-phenylbenzofuran-2-carboxylic acid ethyl ester derivatives as potent anti-tumor agents. Bioorg Med Chem Lett. 2004;14(2):455–8.
12. Creaven BS, Devereux M, Karcz D, Kellett A, McCann M, Noble A, et al. Copper(II) complexes of coumarin-derived Schiff bases and their anti-Candida activity. J Inorg Biochem. 2009;103(9): 1196–203.
13. Creaven BS, Egan DA, Karcz D, Kavanagh K, McCann M, Mahon M, et al. Synthesis, characterisation and antimicrobial activity of copper(II) and manganese(II) complexes of coumarin-6,7-dioxyacetic acid (cdoaH2) and 4-methylcoumarin-6,7-dioxyacetic acid (4-MecdoaH2): X-ray crystal structures of [Cu(cdoa)(phen)2] 8.8H2O and [Cu(4-Mecdoa)(phen)2] 13H2O (phen = 1,10-phenanthroline). J Inorg Biochem. 2007;101(8):1108–19.
14. Creaven B, Devereux M, Georgieva I, Karcz D, McCann M, Trendafilova N, et al. Molecular structure and spectroscopic studies on novel complexes of coumarin-3-carboxylic acid with Ni(II), Co(II), Zn(II) and Mn(II) ions based on density functional theory. Spectrochim Acta A Mol Biomol Spectrosc. 2011;84(1): 275–85.
15. Gudasi KB, Shenoy RV, Vadavi RS, Patil MS, Patil SA. Synthesis, characterisation and biological evaluation of lanthanide(III) complexes with 3-acetylcoumarin-o-aminobenzoylhydrazone (ACAB). Chem Pharm Bull. 2005;53(9):1077–82.
16. Kostova I, Momekov G, Zaharieva M, Karaivanova M. Cytotoxic activity of new lanthanum(III) complexes of bis-coumarins. Eur J Med Chem. 2005;40(6):542–51.
17. Kostova I, Momekov G. New zirconium(IV) complexes of coumarins with cytotoxic activity. Eur J Med Chem. 2006;41(6): 717–26.
18. Kostova I, Kostova R, Momekov G, Trendafilova N, Karaivanova M. Antineoplastic activity of new lanthanide (cerium, lanthanum and neodymium) complex compounds. J Trace Elem Med Biol. 2005;18(3):219–26.
19. Maucher A, Kager M, Von Angerer E. Evaluation of the antitumour activity of coumarin in prostate cancer models. J Cancer Res Clin Oncol. 1993;119(3):150–4.
20. Creaven BS, Egan DA, Kavanagh K, McCann M, Noble A, Thati B, et al. Synthesis, characterization and antimicrobial activity of a series of substituted coumarin-3-carboxylatosilver (I) complexes. Inorg Chim Acta. 2006;359(12):3976–84.
21. Georgieva I, Trendafilova N, Kiefer W, Rastogi V, Kostova I. Vibrational and theoretical study of coumarin-3-carboxylic acid binding mode in Ce(III) and Nd(III) complexes. Vib Spectrosc. 2007;44(1):78–88.
22. Karaliota A, Kretsi O, Tzougraki C. Synthesis and characterization of a binuclear coumarin-3-carboxylate copper(II) complex. J Inorg Biochem. 2001;84(1):33–7.
23. Castellani CB, Carugo O. Studies on fluorescent lanthanide complexes. New complexes of lanthanides(III) with coumarinic-3-carboxylic acid. Inorg Chim Acta. 1989;159(2):157–61.
24. Georgieva I, Trendafilova N, Aquino AJ, Lischka H. Theoretical study of metal-ligand interaction in Sm(III), Eu(III), and Tb(III) complexes of coumarin-3-carboxylic acid in the gas phase and solution. Inorg Chem. 2007;46(25):10926–36.
25. Georgieva I, Trendafilova N, Creaven BS, Walsh M, Noble A, McCann M. Is the CO frequency shift a reliable indicator of coumarin binding to metal ions through the carbonyl oxygen? Chem Phys. 2009;365(1):69–79.
26. Mihaylov T, Trendafilova N, Kostova I, Georgieva I, Bauer G. DFT modeling and spectroscopic study of metal–ligand bonding in La(III) complex of coumarin-3-carboxylic acid. Chem Phys. 2006;327(2):209–19.
27. Roh S-G, Baek NS, Hong K-S, Kim HK. Synthesis and photophysical properties of luminescent lanthanide complexes based on coumarin-3-carboxylic acid for advanced photonic applications. Bull Korean Chem Soc. 2004;25(3):343–4.
28. Ng SW. Coordination complexes of triphenyltin coumarin-3-carboxylate with O-donor ligands:(coumarin-3-carboxylato) triphenyltin–L (L = ethanol, diphenylcyclopropenone and quinoline *N*-oxide) and bis [(coumarin-3-carboxylato) triphenyltin]–L (L = triphenylphosphine oxide and triphenylarsine oxide). Acta Crystallogr C. 1999;55(4):523–31.
29. Ng SW, Kumar DasV. Tetramethylammonium bis (coumarin-3-carboxylato) triphenylstannate ethanol solvate. Acta Crystallogr C. 1997;53(8):1034–6.
30. Mosa A, Emara AA, Yousef J, Saddiq A. Novel transition metal complexes of 4-hydroxy-coumarin-3-thiocarbohydrazone: pharmacodynamic of Co(III) on rats and antimicrobial activity. Spectrochim Acta A Mol Biomol Spectrosc. 2011;81(1):35–43.

31. Köse DA, Sahin O, Büyükgüngör O. Synthesis, spectral, thermal, magnetic and structural study of diaquabis (m-hydroxybenzoato-κO)bis(*N*,*N*-diethylnicotinamide-κN)cobalt(II). Eur Chem Bull. 2012;1(6):196–201.
32. Köse D, Gökçe G, Gökçe S, Uzun I. Bis (*N*,*N*-diethylnicotinamide) p-chlorobenzoate complexes of Ni(II), Zn(II) and Cd(II). J Therm Anal Calorim. 2009;95(1):247–51.
33. Köse DA, Necefoğlu H, Şahin O, Büyükgüngör O. Synthesis, structural, spectroscopic characterization, and structural comparison of 3-hydroxybenzoate and nicotinamide/*N*,*N*′-diethylnicotinamide mixed ligand complexes with Zn(II). J Therm Anal Calorim. 2012;110(3):1233–41.
34. Köse D, Necefoğlu H. Synthesis and characterization of bis(nicotinamide)m-hydroxybenzoate complexes of Co(II), Ni(II), Cu(II) and Zn(II). J Therm Anal Calorim. 2008;93(2):509–14.
35. Nakamoto K. Infrared and Raman spectra of inorganic and coordination compounds. New York: Wiley; 1986.
36. Kose DA, Necefoğlu H, Şahin O, Büyükgüngör O. Synthesis, spectral, thermal and structural study of monoaquabis(acetylsalicylato-κO)bis(nicotinamide-κN)copper(II). J Chem Crystallogr. 2011;41(3):297–305.
37. Köse DA, Ay AN, Şahin O, Büyükgüngör O. A mononuclear, mixed (salicylato)(nicotinamide) complex of Zn(II) with penta- and hexa-coordination sites: a novel framework structure. J Iran Chem Soc. 2012;9(4):591–7.
38. Dağlı Ö, Köse DA, Şahin O, Şahin ZS. The synthesis and structural characterization of transition metal coordination complexes of coumarilic acid. J Therm Anal Calorim. 2017. doi:10.1007/s10973-016-6053-y.
39. Györyová K, Szunyogová E, Kovářová J, Hudecová D, Mudroňová D, Juhaszova E. Biological and physicochemical study of zinc(II) propionate complexes with N-donor heterocyclic ligands. J Therm Anal Calorim. 2003;72(2):587–96.
40. Sheldrick GM. A short history of SHELX. Acta Crystallogr A. 2008;64(1):112–22.
41. Farrugia L. WinGX suite for single crystal small molecule crystallography. J Appl Cryst. 1999;32:837–8.
42. Mercury, version 3.0; CCDC. ccdc.cam.ac.uk/products/mercury. 2016.
43. Spek A. PLATON, a multipurpose crystallographic tool. Utrecht: Utrecht University; 2001.
44. Erel O. A novel automated method to measure total antioxidant response against potent free radical reactions. Clin Biochem. 2004;37:112–9.